

This discussion paper is/has been under review for the journal Biogeosciences (BG).  
Please refer to the corresponding final paper in BG if available.

## Fast and accurate irradiance calculations for ecosystem models

C. D. Mobley<sup>1</sup>, L. K. Sundman<sup>2</sup>, W. P. Bissett<sup>3</sup>, and B. Cahill<sup>4</sup>

<sup>1</sup>Sequoia Scientific, Inc., 2700 Richards Road, Suite 107, Bellevue, WA 98005, USA

<sup>2</sup>Sundman Consulting, 1453 S. Haleyville Circle, Aurora, CO 80018, USA

<sup>3</sup>WeoGeo, 2828 SW Corbett Ave., Suite 135, Portland, OR 97201, USA

<sup>4</sup>Institute of Marine and Coastal Science, Rutgers University, 71 Dudley Road,  
New Brunswick, NJ 08901, USA

Received: 7 October 2009 – Accepted: 28 October 2009 – Published: 16 November 2009

Correspondence to: C. D. Mobley (curtis.mobley@sequoiasci.com)

Published by Copernicus Publications on behalf of the European Geosciences Union.

10625

### Abstract

Coupled physical-biological-optical ocean ecosystem models often use sophisticated treatments of their physical and biological components, while oversimplifying the optical component to the possible detriment of the ecosystem predictions. To bring optical  
5 computations up to the standard required by recent ecosystem models, we developed a computationally fast numerical model, named EcoLight, that solves the azimuthally averaged radiative transfer equation to obtain accurate in-water spectral irradiances for use in calculations of photosynthesis and photo-oxidation. To evaluate its computational features, we incorporated EcoLight into an idealized physical-biological model for  
10 open-ocean Case 1 waters and compared ten-year simulations for a simple analytical irradiance model vs. EcoLight numerical calculations. After optimization, the EcoLight run times are less than 30% more than for the analytical irradiance model. Moreover, EcoLight is suitable for use in Case 2 and optically shallow waters, for which no analytical irradiance models exist. EcoLight also computes ancillary quantities such as the  
15 remote-sensing reflectance, which can be useful for ecosystem validation.

### 1 Introduction

The fundamental measure of light energy in an aquatic system is the spectral radiance  $L$ , which in horizontally homogeneous water bodies is a function of time, depth, direction, and wavelength. In situations relevant to ecosystem modeling, changes in  
20 the water absorption and scattering properties and boundary conditions occur on time scales much longer than needed for the radiance to achieve steady state, and the time dependence can be omitted when solving the radiative transfer equation (RTE). The radiance at any particular time is then  $L(z, \theta, \phi, \lambda)$ , where  $z$  is depth, measured positive downward from  $z = 0$  at the mean water surface;  $\theta$  is the polar angle, with  $\theta = 0$  referring to light traveling toward the nadir ( $+z$ ) direction;  $\phi$  is the azimuthal direction; and  
25  $\lambda$  is the wavelength. (This paper uses the notation and terminology of Mobley, 1994.)

10626

The directional information contained in the radiance is usually irrelevant because water constituents such as phytoplankton and dissolved substances are assumed equally likely to interact with a photon regardless of its direction of travel. Therefore, the spectral scalar irradiance,

$$E_o(z, \lambda) = \int_0^{2\pi} \int_0^\pi L(z, \theta, \phi, \lambda) \sin\theta d\theta d\phi, \quad (1)$$

is the fundamental radiometric quantity necessary for predictions of aquatic primary productivity, photochemical reactions, and heating of water. When modeling photosynthesis, which depends on the number of photons absorbed, it is necessary to multiply  $E_o(z, \lambda)$  by  $\lambda/hc$ , where  $h$  is Planck's constant and  $c$  is the speed of light. This converts the energy units of the spectral irradiance,  $\text{Wm}^{-2}\text{nm}^{-1}$ , to quantum units,  $\text{photons s}^{-1}\text{m}^{-2}\text{nm}^{-1}$ .

A simple measure of the total light available for photosynthesis, the photosynthetically available radiation (PAR),

$$\text{PAR}(z) = \int_{400}^{700} E_o(z, \lambda) \frac{\lambda}{hc} d\lambda, \quad (2)$$

is frequently used in ecosystem models. Some models approximate PAR in terms of the downwelling irradiance  $E_d$ . However, the use of  $E_d$  instead of  $E_o$  in Eq. (2) significantly underestimates PAR (Sakshaug et al., 1997), especially near the surface and in shallow water where upwelling light can significantly contribute to the total irradiance.

Simple analytical models are commonly employed for estimating the dependence of PAR on time (diurnal, inter-day, or seasonal changes), depth, and water inherent optical properties (IOPs, namely the water absorption and scattering properties). Climatological data are often used to provide the time dependence of the (downwelling) surface irradiance. If intraday variability of the light field is included, it is sometimes expressed by a sinusoidal (Bissett et al., 1994) or sawtooth (Evans and Parslow, 1985) function.

10627

Some studies have used astronomical models to estimate the solar radiation as a function of time (Fasham, 1995; Hurtt and Armstrong, 1996), while others neglected the diurnal variation of light completely, using climatological daily-averaged values (Oguz et al., 1996). Errors associated with approximating (or neglecting) temporal variability are greatest when photo-limited and photo-adaptive effects are significant.

Traditionally, coupled ecosystem models have incorporated simple analytical formulas to predict  $\text{PAR}(z)$  from a given chlorophyll profile and from an estimate of PAR at the sea surface (Evans and Parslow, 1985; Fasham et al., 1990; Doney et al., 1996; Hurtt and Armstrong, 1996; Oschlies and Garçon, 1998). Although these analytical PAR models are computationally fast, they can produce estimates that differ by a factor of three near the sea surface and by a factor of ten at the bottom of the euphotic zone (Zielinski et al., 1998). Indeed, the depth of the euphotic zone, if defined as the depth where PAR decreases to one percent of its surface value, differs by almost a factor of two among these models. Errors of this magnitude are unacceptable for quantitative predictions of primary productivity or upper-ocean thermal structure. Additional inaccuracies can be found in the application of the PAR formulas, such as the use of downwelling plane irradiance  $E_d$  as a proxy for the scalar irradiance.

The depth dependence of the irradiance is often expressed as a simple exponential decay function,  $\text{PAR}(z) = \text{PAR}(0)\exp(-K_{\text{PAR}}z)$ , where  $K_{\text{PAR}}$  is an attenuation coefficient for PAR. Kyewalyanga et al. (1992) accounted for the different path lengths associated with direct solar and diffuse light by defining two attenuation coefficients that depend on the mean cosine of the downwelling radiance and on the solar elevation. Some models (Fasham, 1995; Hurtt and Armstrong, 1996; Oguz et al., 1996; Moore et al., 2002) consider the contributions to the attenuation by different components (pure water, chlorophyll, CDOM, etc.), but still neglect the spectral dependence of the attenuation of light. Most assume that the attenuation rates of each component are constant with depth (Evans and Parslow, 1985; Fasham, 1995; Hurtt and Armstrong, 1996; Oguz et al., 1996; Kyewalyanga et al., 1992). Others use depth-averaged values (Doney et al., 1996). Moore et al. (2002) use a depth-averaged PAR value within the mixed

10628

layer. Such simplifications can induce significant errors, especially near the surface where the spectral distribution of the light field is changing rapidly with depth as the water preferentially absorbs some wavelengths while transmitting others. Errors generated near the surface propagate with depth and thereby influence on the light field throughout the euphotic zone.

Many papers set the PAR value just below the surface to be 45–52% of the total solar illumination, citing Baker and Frouin (1987). However, Baker and Frouin reported ratios of the downwelling plane irradiance in the 400–700 nm range just above the surface to the total solar illumination (plane irradiance) at the top of the atmosphere. Their work studied the sensitivity of this ratio to atmospheric conditions. They did not consider scalar irradiances or PAR and they did not study the transmittance of the light through the sea surface.

Simpson and Dickey (1981) investigated the sensitivity of the total downwelling irradiance over the entire spectrum as estimated from five models to a number of factors. They divided the models into categories based on the mathematical form of the models: simple exponential, bimodal, arctangent, and multiband. Zielinski et al. (1998) also used these categories to evaluate the influence of PAR models by applying them to a set of ESTOC (European Station for Time-series in the Ocean Canary Islands; located at 29°10' N, 15°30' W) data and a one-dimensional (depth dependent) bio-physical model. They quantified the effect of the variation between the different PAR models. However, conclusions about the influence of PAR on their coupled model were somewhat limited by the absence of measurements of the actual PAR.

Although simple PAR models are computationally convenient, any ecosystem model based on PAR is limited in its realism, regardless of how accurately PAR is computed. Different species of phytoplankton have different pigment suites, which respond differently to different wavelengths. Therefore, any model that attempts to describe competition between different species or functional groups having different pigments must use spectral irradiance, not a wavelength-integrated measure of the light.

The Ecosystem Simulation (EcoSim) model of Bissett et al. (1999a,b) moves beyond

10629

PAR calculations and calculates and uses the spectral distribution of light. EcoSim includes four phytoplankton functional groups, each with a characteristic pigment suite that changes over time with light and nutrient conditions. To model light effects on changes within and competition between these groups, EcoSim uses an approximate model for the spectral scalar irradiance in Case 1 waters (described below). The spectral irradiance is used with the modeled pigment suites to create competition among phytoplankton groups based on their photosynthetic action spectra. In addition to dealing explicitly with spectral light and its impacts on phytoplankton community structure, EcoSim also explicitly models the feedbacks from changes in IOPs, e.g. CDOM photolysis and photoacclimation of phytoplankton, which in turn drive changes in the color and intensity of light at depth. Although the EcoSim spectral irradiance model is sufficiently fast for use in coupled physical-biological ecosystem simulations involving many grid points and time steps, it does rest on several approximations that can limit its accuracy even in Case 1 waters, and it is not applicable to Case 2 or optically shallow waters.

There is today much interest in the modeling of coastal waters, which are often Case 2 due to resuspended sediments or terrigenous particles and dissolved substances, and which may be shallow enough for bottom reflectance to make a significant contribution to the scalar irradiance. If EcoSim or similar models are to accurately simulate such optically complex waters, they must incorporate spectral irradiance models that are computationally fast, accurate, and applicable to any water body. To address this need, we have developed a specialized version of the HydroLight radiative transfer model (Mobley et al., 1993; Mobley, 1994, and <http://www.hydrolight.info>), called EcoLight, which is designed to bring the optical component of ecosystem models up to the level of sophistication found in the latest physical and biological models. Fujii et al. (2007) incorporated an early version of EcoLight into a physical-biological model and showed that improved optical calculations help constrain ecosystem behavior and gave predictions consistent with observations in simulations of an equatorial Pacific upwelling region. They however did not consider ways of optimizing the EcoLight calcula-

10630

tions to preserve accuracy while minimizing run times, nor did they compare long-term ecosystem behavior for simple vs. accurate light calculations.

We incorporated EcoLight into a coupled model and compared its performance with the spectral irradiance model used in EcoSim. We first briefly describe the physical and biological models, and then EcoLight and the coupled model. We then compare the predictions made for an idealized ecosystem simulation when using the original EcoSim light model with those made using various EcoLight options.

## 2 The ecosystem model

Our ecosystem model has separate submodels for the physical, biological, and optical components, which we describe next.

### 2.1 The ROMS physical model

The physical model used here is the Regional Ocean Modeling System (ROMS). ROMS is widely used for coastal and shelf circulation and coupled physical-biological applications (e.g. Dinniman et al., 2003; Lutjeharms et al., 2003; Marchesiello et al., 2003; Peliz et al., 2003; Fennel et al., 2006, 2008; Fennel and Wilkin, 2009; Wilkin, 2006; Cahill et al., 2008). The ROMS computational kernel (Shchepetkin and McWilliams, 1998, 2003, 2005) produces accurate evolution of tracer fields, which is a particularly attractive feature for biogeochemical modeling because it facilitates accurate interaction among tracers and accounting of total nutrient and carbon budgets.

The present study uses a 6×6 horizontal grid domain with periodic lateral boundary conditions. This spatially limited domain was chosen to minimize run times during the EcoLight code development and evaluation simulations. For the simulations presented below, the grid is centered off the continental shelf of the eastern United States near 73.2° W and 38.8° N, as shown in Fig. 1. The horizontal grid resolution is approximately 10 km. The vertical grid has 30 points covering the upper 210 m of the water column;

10631

the vertical resolution ranges from approximately 2 m near the sea surface to 15 m at depth.

In our simulations the ROMS model was driven by an annual cycle of external irradiances and winds obtained from reanalysis of gridded atmospheric data at 6-hour resolution obtained from the European Centre for Medium-Range Weather Forecasts. Water column heating as needed to compute mixed layer dynamics in ROMS is obtained from simple analytical models for band-integrated short and long-wave radiation. Figure 2 shows the daily local-noon short-wave irradiances used as inputs to ROMS. This same annual cycle was repeated for each simulation year.

### 2.2 The EcoSim biological model

EcoSim is an ecological-optical modeling system that was developed for simulations of carbon cycling and biological productivity (Bissett et al., 1999a,b, 2005, 2008). It includes four phytoplankton functional groups (FG1 is small diatoms, FG2 is large diatoms, FG3 is large dinoflagellates, and FG4 is *synechococcus*), each with a characteristic pigment suite that varies with the group carbon-to-chlorophyll *a* ratio, C:Chl*a*. EcoSim spectrally-resolves the irradiance as opposed to using wavelength-integrated irradiance. This allows differential growth of different phytoplankton groups that have unique pigment suites. The properties of each functional group evolve over time as a function of light and nutrient conditions. Other EcoSim components include bacteria, dissolved organic matter, dissolved inorganic carbon cycling and 5 nutrients (NO<sub>3</sub>, NH<sub>4</sub>, PO<sub>4</sub>, SiO, and FeO). The interactions between EcoSim's components describe autotrophic growth of and competition between the four phytoplankton groups, differential carbon and nitrogen cycling, nitrogen fixation, and grazing. The maximum phytoplankton growth is modulated by temperature (Eppley, 1972). Loss is effected by grazing and excretion. Grazing accounts for the majority of the biomass sink in this model and is considered the closure term of the phytoplankton equations (Steele and Henderson, 1992). Grazing is modeled as a Michaelis-Menten function based on the functional groups' biomass (Bissett et al., 1999a). The initial application of EcoSim

10632

to predictions of seasonal cycles of carbon cycling and phytoplankton dynamics in the Sargasso Sea showed that its predictions were consistent with measurement of various biological and chemical quantities at the Bermuda Atlantic Time-series Study (BATS) station (Bissett et al., 1999a).

5 EcoSim version 2.0 as used in the present simulations includes nutrient recycling to replenish nutrients lost as particles sink below the bottom of the maximum simulation depth. Fecal material and phytoplankton sink at various rates:  $0.01 \text{ mday}^{-1}$  for FG1,  $0.1 \text{ mday}^{-1}$  for FG2,  $10 \text{ mday}^{-1}$  for fecal material, and no sinking for FG3, FG4 and dissolved components. When particles reach the maximum depth, their masses are  
10 converted to nutrients as follows: fecal and phytoplankton carbon are converted to dissolved inorganic carbon, fecal and phytoplankton nitrogen are converted to  $\text{NO}_3$ , phosphorous is converted to  $\text{PO}_4$ , silicon to  $\text{SiO}$ , and iron to  $\text{FeO}$ . The flux of nutrients out of the bottom of the model domain is immediately converted into a corresponding influx of nutrients into the bottom of the model domain. Other modifications to EcoSim  
15 since its original publication are described in Bissett et al. (2004).

The absorption spectra of the phytoplankton functional groups change with light and nutrient adaptation. The four groups therefore respond differently to various wave-  
lengths of the available light, and each group responds differently over time. EcoSim requires spectral irradiances at 5 nm bandwidths between 400 and 700 nm in order  
20 to model the changes within each functional group and competition between them. The use of spectral irradiance rather than broadband PAR in modeling phytoplankton dynamics is a distinguishing feature of EcoSim. The standard EcoSim code, which we call the analytic light (AL) version, first calls the RADTRAN (Gregg and Carder,  
1990) atmospheric radiative transfer model to obtain the spectral downwelling direct and diffuse plane irradiances just beneath the sea surface for clear sky conditions.  
25 These clear-sky irradiances are functions of the atmospheric conditions (aerosol type, humidity, etc.) and solar zenith angle. The model can be driven by measured or climatological sea surface PAR measurements. When this is done, PAR computed from the RADTRAN spectrum is compared with the measured PAR, and the PAR ratio is

10633

used to rescale the computed spectral irradiances at the sea surface. In the present simulations, the wavelength-integrated RADTRAN irradiances are rescaled to give the current value of the ROMS short-wave irradiance as shown in Fig. 2.

The RADTRAN-computed and rescaled spectral downwelling plane irradiances just  
5 beneath the sea surface are then propagated to depth using

$$E_d(z, \lambda) = E_d(0, \lambda) \exp \left[ - \int_0^z K_d(z', \lambda) dz' \right] \quad (3)$$

and a simple model for  $K_d$ ,

$$K_d(z, \lambda) = \frac{a(z, \lambda) + b_b(z, \lambda)}{\bar{\mu}_d(z, \lambda)}. \quad (4)$$

Here  $a(z, \lambda)$  is the total absorption coefficient (the sum of absorption by pure water and  
10 the various particulate and dissolved components), and  $b_b(z, \lambda)$  is the total backscatter coefficient. The phytoplankton absorption is obtained from the concentrations of the functional groups and their chlorophyll-specific absorption spectra. The backscatter coefficient is obtained from the chlorophyll-dependent model of Morel and Maritorena (2001) for Case 1 waters, using the total Chl *a* concentration. The total scattering coefficient  $b(z, \lambda)$  is obtained from the Case 1 model of Gordon and Morel (1983). The mean cosine for downwelling irradiance,  $\bar{\mu}_d(z, \lambda)$ , is itself modeled by a simple function  
15 that merges estimates of the near-surface and asymptotic-depth mean cosines (Bissett et al., 1999b, Eqs. 18–22). The value of  $\bar{\mu}_d$  at the surface is set to the cosine of the in-water solar zenith angle; the value at the maximum depth is set to 0.75, which is a  
20 typical value for oceanic asymptotic light fields. Finally, the needed scalar irradiance  $E_o(z, \lambda)$  is obtained from the computed  $E_d(z, \lambda)$  and the approximation

$$E_o(z, \lambda) \approx \frac{E_d(z, \lambda) K_d(z, \lambda)}{a(z, \lambda)}. \quad (5)$$

10634

EcoSim AL uses Eqs. (3–5) to compute the irradiance to a depth at which  $E_o(z, \lambda)$  integrated from 400 to 700 nm becomes less than  $1 \text{ Wm}^{-2}$ .

In the  $6 \times 6$  grid ROMS-EcoSim code, the outer layer of grid points seen in Fig. 1 is used to impose the periodic boundary conditions. Therefore the EcoSim code computes the biology only at the interior  $4 \times 4$  block of grid points. The biology is updated at each ROMS time step and interior grid point using the analytic formulas for the scalar irradiance just described. However, the irradiances computed within EcoSim do not feed back to the ROMS code which, for programming simplicity when merging the codes, retains its original short and long-wave light parameterization for mixed-layer heating calculations. Thus the physical model influences the biology via temperature and mixing, but the optical model employed within EcoSim does not influence the physical model. This simplification was retained in the present study to avoid alterations to the ROMS code.

### 2.3 The EcoLight radiative transfer model

Accurate predictions of primary production require accurate predictions of the ambient spectral scalar irradiance. Numerical models that solve the scalar RTE are currently available (Mobley et al., 1993) and can provide highly accurate predictions of the light field, in particular the scalar irradiance as a function of depth and wavelength. However, the computational times required by these numerical models are far too great for their inclusion in large coupled models that need irradiance predictions at many spatial locations and times of day.

The HydroLight radiative transfer model (Mobley et al., 1993; Mobley, 1994, and [www.hydrolight.info](http://www.hydrolight.info)) provides an accurate solution of the scalar RTE for any water body, given the inherent optical properties of the water body, the incident sky radiance, and the bottom reflectance (in finite-depth waters). Although the standard version of HydroLight is computationally very efficient, its run times are still much too long for use in ecosystem models. HydroLight computes the radiance for a set of  $M$  polar directions and  $N$  azimuthal directions. The total number of directions is then  $(M - 2)N + 2$ ;

10635

namely  $N$  azimuthal angles for each non-polar-cap direction, plus the zenith and nadir polar cap directions. The computational time is proportional to this number of directions squared, because each direction interacts via scattering with every other direction. A large part of the HydroLight run time is used to compute the azimuthal dependence of the radiance distribution. A slightly optimized version of HydroLight 3.1 was developed by Liu et al. (1999). Liu et al. (2002) developed a multi-parameter look-up-table for scalar irradiance in homogeneous waters. Their model is based on HydroLight simulations and gives PAR profiles that are within a few percent of HydroLight values but runs four orders of magnitude faster. However, the Liu et al. (2002) model is not suited to the needs of EcoSim when modeling inhomogeneous or Case 2 waters.

Ecosystem models require only the scalar irradiance  $E_o$  as a function of depth and wavelength, which is computed from an azimuthal integration of the radiance as seen in Eq. (1). The azimuthal dependence of the radiance, obtained at great computational expense in HydroLight, is thus lost in the integration of Eq. (1). This means that the RTE can be azimuthally averaged to obtain an equation for the azimuthally averaged radiance as a function of polar angle. The numerical solution of the resulting RTE is much simpler than in HydroLight. In particular, there is no azimuthal decomposition of the radiance into Fourier amplitudes. Only  $M$  azimuthally averaged radiances need be computed, and the run time is proportional to  $M^2$ . The standard version of HydroLight uses  $M = 20$   $\theta$  directions and  $N = 24$   $\phi$  directions, which gives 10 degree resolution in the polar angle (including two polar caps with 5 degree half-angles) and 15 degree resolution in the azimuthal angle. Eliminating the azimuthal dependence from the calculations therefore gives approximately a factor-of-400 reduction in the computation time (allowing for certain calculations that are independent of angular resolution).

Based upon this observation, we developed a highly optimized version of HydroLight 4.2, called EcoLight, which solves the azimuthally averaged RTE as a function of depth and wavelength for any water body. EcoLight requires the same IOP and boundary condition inputs as HydroLight, and the resulting irradiances are computed with the same accuracy as HydroLight. Related quantities such as the irradiance reflectance,

10636

nadir-viewing water-leaving radiance and remote-sensing reflectance, and diffuse attenuation coefficients also computed by EcoLight. Although those ancillary quantities are not needed as inputs to most ecosystem models, they can be of use in ecosystem model validation. In particular, the water-leaving radiance and remote-sensing reflectance allow ecosystem validation using satellite radiometric measurements without the intervening step of converting radiometric measurements into chlorophyll concentrations via imperfect chlorophyll algorithms. Quantities such as the remote-sensing reflectance are not available from the simple analytic light models.

Various additional optimizations to the EcoLight code were made. The most important are the use of a piecewise homogeneous water column, solution of the RTE to different depths at different wavelengths, and wavelength skipping.

The ROMS-EcoSim code models the water column as a stack of homogeneous layers of variable thickness. Therefore the IOPs within a given water layer are independent of depth. The EcoLight code takes advantage of the depth independence of the IOPs within a layer to reduce the computation needed to solve the RTE for the depth dependence of the irradiances within each layer.

HydroLight solves the RTE to a user-specified geometric depth, which is the same for every wavelength and must be chosen before the run is started. This becomes computationally expensive at wavelengths where the IOPs are large (e.g., at red wavelengths owing to pure water absorption or at blue wavelengths owing to CDOM absorption) corresponding to a large optical depth for a given geometric depth. EcoSim requires the spectral scalar irradiance only to the bottom of the euphotic zone, below which it does not perform primary production calculations. Therefore, it is necessary to compute the irradiance only to that depth, which varies with the biological state of the ocean and cannot be predetermined.

In EcoLight the goal is to solve the RTE to the shallowest depth possible and then to extrapolate the scalar irradiance to greater depths. To determine the depth to which the RTE is to be solved at a particular wavelength, an equation of the form of Eq. (3) can be written using  $E_o$  instead of  $E_d$  and  $K_o$  instead of  $K_d$ . Note that  $K_o$  is an apparent

10637

optical property and is not known until the RTE has been solved. However, except very near the sea surface where boundary effects are important,  $K_o$  is roughly equal to  $K_d$ , the diffuse attenuation coefficient for downwelling plane irradiance ( $K_o$  becomes exactly equal to  $K_d$  at great depths in homogeneous water). To first order (e.g., Mobley, 1994, Eq. 5.65)  $K_d \approx a/\bar{\mu}_d$ , where  $a$  is the absorption coefficient and  $\bar{\mu}_d$  is the mean cosine of the downwelling radiance distribution. In typical waters,  $\bar{\mu}_d \approx 3/4$ . Thus, in the modified Eq. (3) we can approximate  $K_o(z, \lambda)$  by the absorption coefficient  $a(z, \lambda)$  and define

$$F_o \equiv \frac{E_o(z_o, \lambda)}{E_o(0, \lambda)} \approx \exp \left[ - \int_0^{z_o} a(z', \lambda) dz' \right]. \quad (6)$$

Given the absorption coefficient, which is known before the RTE is solved, this equation can be used to estimate the depth  $z_o$  at which the scalar irradiance will decrease to a fraction  $F_o$  of its surface value. Because of the approximations used, the estimated  $z_o$  will always be greater than the actual  $z_o$ .

At the first wavelength,  $z_o$  is obtained from Eq. (6) for a pre-specified  $F_o$ , and the bottom boundary condition is then applied at this depth. At the first wavelength,  $\lambda_1$ , the RTE is solved to the estimated depth,  $z_o(\text{est}; \lambda_1)$ , determined as just described. After the RTE is solved, the actual depth  $z_o(\text{exact}; \lambda_1)$  at which  $E_o(z, \lambda_1)$  decreased to  $F_o E_o(0, \lambda_1)$  can be determined. At subsequent wavelengths, the ratio of actual to estimated  $z_o$  values from the previous wavelength is used to correct the initial estimate at the present wavelength:

$$z_o(\text{final}; \lambda_j) = z_o(\text{est}; \lambda_j) \frac{z_o(\text{exact}; \lambda_{j-1})}{z_o(\text{est}; \lambda_{j-1})}. \quad (7)$$

Thus, if the initial absorption-based estimate of  $z_o$  at the previous wavelength was 20% too large, it is assumed that the initial estimate at the current wavelength is also 20% too large, and the initial estimate of  $z_o$  is reduced accordingly. This adjustment, which is based upon the exact depth at the previous wavelength, corrects for the error

10638

inherent in Eq. (6) because  $K_o$  was approximated by  $a$ . Numerical studies show that after the first wavelength, which always goes too deep, this algorithm gives final depth estimates that are close to the actual  $F_o$  depths, as determined after solving the RTE. In practice, the RTE is solved to the next depth  $z_k > z_o$ , where  $z_k, k = 1, \dots, 30$  is one of the ROMS-EcoSim grid depths.

The computed values of  $E_o(z_k)$  and  $E_d(z_k)$  are then accurate down to depth  $z_k$ , and they can be extrapolated to greater depths as follows. The extrapolation is based on Eq. (3), except that the mean cosine factors can now be included in the approximations for  $K_d \approx a/\bar{\mu}_d$  and  $K_o \approx a/\bar{\mu}$ .

In addition to  $E_o(z_k, \lambda)$  and  $E_d(z_k, \lambda)$ , the solution of the RTE gives all irradiances, in particular the downwelling scalar irradiance  $E_{od}(z_k, \lambda)$  and the upwelling plane irradiance  $E_u(z_k, \lambda)$ . These irradiances are used to compute

$$\bar{\mu}_d(z_k, \lambda) = \frac{E_d(z_k, \lambda)}{E_{od}(z_k, \lambda)} \quad \text{and} \quad \bar{\mu}(z_k, \lambda) = \frac{E_d(z_k, \lambda) - E_u(z_k, \lambda)}{E_o(z_k, \lambda)}$$

at the last solved depth. These values of  $\bar{\mu}_d$  and  $\bar{\mu}$  at depth  $z_k$  are then used at all lower depths. Thus Eq. (3) written for  $E_o$  becomes

$$E_o(z, \lambda) = E_o(z_k, \lambda) \exp \left[ - \int_{z_k}^z \frac{a(z', \lambda)}{\bar{\mu}(z_k, \lambda)} dz' \right]. \quad (8)$$

A similar equation using  $\bar{\mu}_d(z_k, \lambda)$  holds for  $E_d$ . Equation (8) is then applied to the homogeneous layers beginning at depth  $z_k$  and extending to the maximum depth of the ROMS-EcoSim grid.

Note that  $E_o(z_k, \lambda)$  and the other irradiances incorporate all of the effects of the surface boundary and of the water IOPs above the maximum depth  $z_k$  to which the RTE was solved. The extrapolations based on Eq. (8) are accurate if the variability in the  $\bar{\mu}$  factors is not great below depth  $z_k$  and if the attenuation covaries with the absorption coefficient.

10639

There is also an option to solve the RTE at only some wavelengths and to obtain the irradiances at the unsolved wavelengths (needed by EcoSim) by interpolation. For example, EcoLight can solve the RTE at wavelengths 1, 3, 5... and then estimate the irradiances at wavelengths 2, 4, 6... by interpolation between the computed wavelengths. Omitting every other wavelength gives a factor-of-two decrease in the EcoLight run time, all else being equal.

In summary, EcoLight takes the following philosophy. It is necessary to solve the RTE in order to incorporate the effects of the surface boundary conditions and to account for all IOP effects. However, once an accurate value of  $E_o(z_k, \lambda)$  has been computed to some depth  $z_k$  deep enough to be free of surface boundary effects, it is not necessary to continue solving the RTE to greater depths, which is computationally expensive. As shown below, in many cases of practical interest it is possible to extrapolate the accurately computed upper-water-column irradiances to greater depths and still obtain irradiances that are acceptably accurate for ecosystem predictions. Likewise, it may not be necessary to solve the RTE at every wavelength in order to obtain acceptably accurate irradiances at the needed wavelength resolution.

#### 2.4 The ROMS-EcoSim-EcoLight coupled model

The ROMS and EcoSim models were previously coupled and that code served as the starting point for the incorporation of EcoLight. The analytic irradiance model found in the standard EcoSim code was replaced by a call to the EcoLight subroutine. EcoSim passes EcoLight the current total IOPs as functions of depth and wavelength, atmospheric conditions (as needed by RADTRAN, which is also used by EcoLight to compute the spectral irradiance incident onto the sea surface), wind speed, grid depths, and other information needed by EcoLight. After solving the RTE, EcoLight returns the scalar irradiance  $E_o(z, \lambda)$  to EcoSim for use in its primary production calculations. The remote-sensing reflectance, downwelling and upwelling plane irradiances, mean cosines, and various other quantities are also returned and are archived for post-run analysis.

10640



### 3 Ecosystem behavior

Figure 3 shows the initial chlorophyll vs. depth profiles for the four phytoplankton functional groups. These profiles were used as the “baseline” initial profiles for all subsequent simulations.

5 We first investigated EcoSim’s biological predictions when using its original analytic irradiance model. We expect that the long-term ecosystem behavior should be determined by the ecosystem internal structure and external forcing, and thus be independent of the initial conditions. To verify this, runs were made starting with the initial chlorophyll profiles seen in Fig. 3, and with profiles that were one-half, twice, and  
10 five-times the values seen in that figure. Figure 4 shows the resulting total chlorophyll concentrations (the sums of the chlorophyll concentrations for the four phytoplankton functional groups) near the sea surface for simulation year 1. For this and subsequent figures, values are plotted daily at local noon. As expected, the differences due to the initial chlorophyll profiles damp out within a few months and remain small during  
15 subsequent years. Greater depths show the same behavior, as do runs using EcoLight-computed irradiances.

We next examined the ecosystem annual cycle for long-term simulations. A run for ten simulated years was made starting with the chlorophyll profiles of Fig. 3. The first three years show transient behavior as the ecosystem adjusts to the initial profiles and  
20 external forcing. Years 4–10 then show similar annual cycles, except for a slow year-to-year decrease in chlorophyll concentrations, as shown in Fig. 5. During simulation years 8 to 10, the year-to-year decrease in the annual maximum chlorophyll values is 9 to 11% for diatoms and 3 to 5% for *dynoflagellates* and *synechococcus*, which gives an annual decrease of about 9% in the maximum total chlorophyll. The annual average  
25 chlorophyll values decrease somewhat less over the same three years, with the annual average total chlorophyll (shown by horizontal dotted lines in the figure) decreasing by 6.6 to 6.7% each year. This year-to-year decrease in chlorophyll values is a consequence of imperfect nutrient replenishment as parameterized by the sinking rates and

10641

recycling used in EcoSim. The same behavior occurs with EcoLight irradiance calculations. Such behavior is not surprising for the limited spatial grid (which does not include horizontal advection of nutrients) and fixed particle sinking and nutrient recycling rates assumed here. The failure of the present idealized ecosystem to attain a completely  
5 stable annual cycle in no way compromises our comparisons of analytic vs numerical irradiance calculations, for which all else is the same. Although we do not expect to reproduce local conditions within the limited spatial domain, it is encouraging to note that our modeled surface chlorophyll values in spring-early summer are of the same order of magnitude ( $1\text{--}3\text{ mgm}^{-3}$ ) as coincident SeaWiFs data for this area.

### 10 4 Irradiance model comparisons

We now consider the long-term ecosystem behavior for different ways of computing the scalar irradiance used in EcoSim for its primary production calculations. In these simulations, the time step was 9 min, which was set by ROMS for computational stability. A one-year simulation thus requires 58 400 time steps. In the baseline simulations,  
15 EcoSim updates its light and biology at each time step, although the irradiances are computed only when the sun is above the horizon. Such frequent de novo recomputation of the in-water irradiance is not computationally feasible for EcoLight because of its longer run times, nor is it necessary.

Figure 6 shows a one-year simulation with three versions for the light model called  
20 by EcoSim. The first model is the default analytic light (AL) model used by EcoSim. This model computes the irradiances at every grid point (notation: EGP) and every time step (ETS) when the sun is above the horizon. Irradiances are computed at 5 nm resolution between 400 and 700 nm. Irradiances are computed down to the depth where the integrated  $E_d$  is  $1\text{ W m}^{-2}$ . This is the AL baseline run, which is our standard  
25 for comparison with runs that call the EcoLight model to obtain the irradiances. This AL run required 32 min on a 2.16 GHz Intel Core Duo iMac running OSX with 1 GB RAM. All run times are totals for the ecosystem simulation and include the physical (ROMS),

10642

biological (EcoSim) and optical (analytic or EcoLight) calculations.

The second model uses EcoLight (EL) to compute the irradiances at every grid point, every time step, and every wavelength down to a depth where the scalar irradiance decreased to 0.001 of the surface value, i.e., to a depth  $z_o$  corresponding to  $F_o = 0.001$  in Eq. (6), as dynamically corrected by Eq. (7). For the initial chlorophyll profiles seen in Fig. 3,  $z_o$  is approximately 50 m. Below depth  $z_o$  EcoLight extrapolated the irradiances using Eq. (8). This extrapolation defines the irradiances throughout the water column (down to 210 m in these simulations), even though the values at great depths are not used by EcoSim. These EcoLight computations thus give highly accurate irradiances throughout the euphotic zone, for the IOP and sky inputs passed to EcoLight by ROMS and EcoSim. This full EcoLight simulation corresponds almost exactly to the baseline conditions of the EcoSim calculations using its analytic light model. However, this run required 135 h and 35 min, which is much too long for routine calculations.

The third run shown in Fig. 6 shows the results when EcoLight was called at only one grid point (1GP) and once per simulation hour (1HR), with other options being the same as in the previous EcoLight run. At time steps where EcoLight is not called, the most recently computed spectral irradiances are simply rescaled by the ratio of the current RADTRAN sky irradiance to that at the time of the previous full computation. This should give good irradiances if the IOPs have not changed greatly since the last full calculation. The irradiances at the computed grid point are rescaled in the same manner and applied at the other grid points. This should give reasonably good predictions if the IOPs are not greatly different between the grid points where the exact computation is made and where the rescaled irradiances are applied. This run required 8 h and 34 min, which although much faster than the full EL run is still too long for ecosystem modeling.

As Fig. 6 shows, the AL base and two EL runs differed by as much as 42% during the course of the year (computed as  $100|AL - EL|/AL$ ). However, the EL full and EL 1GP, 1HR (labeled EL base in the figure) runs were always within one percent of each other and are almost indistinguishable in the figure. This shows that EcoLight

10643

can be called at only one grid point and once per hour without significantly altering the ecosystem behavior compared to calling it at every ROMS grid point and every time step. Compared to the EL full model, the EL 1GP, 1HR, 5 nm,  $F_o = 0.001$  run gives the same predictions as the EL full model, but at only 6% of the run time. We therefore adopt these EL options as the baseline for subsequent EcoLight runs for ten-year simulations. We presume that the EL runs give a better ecosystem prediction than the AL run because the EL irradiances are computed more accurately.

Figure 7 shows several comparisons of AL and EL runs during simulation year 10. We first note the similarity between the AL and EL base runs. (The first year of this simulation was seen in Fig. 6.) These two runs differ by no more than 23% after ten years of simulation. This is a relatively small difference given the much different ways in which the irradiances are computed. The similarity in these two runs can be viewed in either of two ways. First, the agreement is a validation of EcoSim's simple analytic irradiance model for Case 1 water, compared to the exact solution of the RTE for the same IOPs. Good agreement is to be expected, since the AL light model was designed for use in Case 1 waters as modeled here. Alternatively, the similarity can be viewed as confirmation that the EcoLight code has been fully debugged and properly embedded within the ROMS-EcoSim code.

Since we can reduce the spatial and temporal frequency of calling EcoLight (or the analytic light model, for that matter) as just described without altering the ten-year ecosystem predictions by more than one percent, the question arises as to how much more the frequency of light computations can be reduced without significantly altering the long-term ecosystem behavior. Figure 7 shows two further examples of reduced temporal, wavelength, and depth resolution in EcoLight runs for the last year of a ten-year simulation. EL Run A called EcoLight at the first ROMS time step after sunrise and every 4 h (4HR) thereafter each day. Irradiances were computed only at every fifth EcoSim waveband, i.e. at 400, 425, ..., 700 nm, which is 25 nm resolution. Irradiances at other EcoSim bands were obtained from linear interpolation between the computed bands. Finally, the RTE was solved only down to the 15% light level, i.e., down to

10644

$F_o = 0.15$ , with extrapolation to deeper depths as previously described. In a similar fashion, EL Run B called EcoLight every 6 h at 50 nm resolution, and solved the RTE down to only the 50% or  $F_o = 0.5$  light level.

The EL base and EL Run A simulations differ by a maximum of 4% during the tenth simulation year. Thus very little long-term difference was induced by the reduction in wavelength and depth resolution for EL Run A vs. the EL base run. However, EL Run A took only 41 min per simulation year, which is just 28% more than the AL base run. EL Run B took 40 min. The small decrease in run time between EL Run A and Run B indicates that the overhead required to call and initialize EcoLight now dominates its run time, rather than the time required to solve the RTE itself. However, EL Run B gives chlorophyll predictions that differ by as much as 73% after ten years, compared to the EL base run. Note also that the time of the maximum spring bloom is delayed by almost a month in EL Run B. Such differences are too large to be acceptable. Thus we view the computational frequency of EL Run A as being satisfactory, given the small increment in run time compared to the AL model, but EL Run B is not satisfactory and in any case gives only a slight additional saving in run time.

The same behavior is seen at greater depths. Figure 8 shows the year-ten time series at depth 15.7 m. At this depth, AL base and EL base differ by up to 26%. EL base and EL run A remain within 4% of each other, but EL Run B differs from Run A by up to 65%. Figure 9 shows the upper 50 m depth profile of total chlorophyll values at day 180 of year 10, illustrating that the largest difference between the analytical and EcoLight model predictions occurs in the upper 20 m. Below this depth, both solutions converge. Table 1 summarizes these runs.

## 5 Conclusions

It is of course possible to try other combinations of time, wavelength, and depth resolution in EcoLight calls, and we have done so. However, the results presented in Figs. 7–9 are sufficient to show that accurate irradiance calculations can be obtained

10645

in ecosystem models with at most a few tens of percent increase in total run times. Although both the analytic and EcoLight models gave comparable chlorophyll predictions for ten-year simulations of open-ocean Case 1 waters, such agreement cannot be expected in simulations of Case 2 waters, for which the analytic light model is not valid. The EcoLight solution of the RTE to a given optical depth is not dependent on whether the IOPs describe Case 1 or 2 water. Its fast run times seen here will therefore be retained in applications to other water bodies. A chlorophyll-based analytic light model will underestimate the scalar irradiance in simulations of optically shallow waters with bright reflective bottoms. In such waters, bottom reflectance increases the in-water scalar irradiance and proportionately affects biological productivity and water-column heating rates. In optically shallow waters, it would be necessary to force EcoLight to solve the RTE all the way to the physical bottom at each wavelength in order to account for bottom reflectance effects. However, any corresponding increase in run time is a penalty worth paying if the improved irradiance computations give significantly better ecosystem predictions in such waters, and the run time will even decrease if the bottom depth is less than the deep-water  $z_o$  given by Eq. (7).

It is our view that it does not matter how fast a light model runs if its predictions are not sufficiently accurate to meet the user's needs. EcoLight provides a numerical light model that accurately computes irradiances for any water body or boundary conditions being simulated by the associated physical-biological models. The run time increase when using EcoLight in an optimized way, i.e., not calling it at every time step, every grid point, and every wavelength, is at most a few tens of percent. Moreover, EcoLight automatically provides ancillary output (not shown in this paper) such as the remote sensing reflectance, plane irradiances, and nadir- and zenith-viewing radiances, all of which can be used to verify ecosystem predictions with observational data, or which may be of use for other purposes such as estimation of underwater visibility. Such ancillary data are not provided by the analytic light model. The use of an RTE-based optical model also facilitates data assimilation into the ecosystem model when IOP or related measurements are available. EcoLight's extra computational time is a small

10646

price to pay for potential improvements in ecosystem predictions, for extending the light model to Case 2 and shallow waters, and for obtaining ancillary radiometric variables useful for ecosystem validation.

We thus feel that although simple analytic irradiance models do run extremely fast, there is little justification for their continued use in light of their potential inaccuracies and limitations, even for Case 1 waters. Moreover, analytic models usually parameterize the water inherent optical properties in terms of a single quantity – the total chlorophyll concentration – which oversimplifies the complex relation between light propagation and the scattering and absorption properties of various ocean constituents. Sophisticated ecosystem models such as EcoSim track several phytoplankton functional groups as well as other dissolved and particulate constituents, each of which has its own absorption and scattering properties. EcoSim determines total inherent optical properties as sums of the contributions by various components and is thus able to model changes in the light field induced by changes in the concentration or optical properties of whatever components are included in the biological model. Such connections between ecosystem components and the light field cannot be well simulated by chlorophyll-based models.

Computational stability criteria of ecosystem physical models may require time steps as small as one minute, depending on grid cell size. However, it is seldom if ever necessary to update the light field at each time step. It appears reasonable to run EcoLight at hourly or longer intervals and then interpolate to the desired time. The same idea applies to running EcoLight on a coarser spatial grid than the physical model uses and then interpolating to obtain the required spatial resolution. In practice, it should be possible to dynamically determine when to call EcoLight. For example, as the calculations proceed to a new grid point, the IOPs at that grid point could be compared with those at the last grid point where EcoLight was called (the reference point). If the IOPs at the new grid point differ by less than some amount from those at the reference point, then the previously computed irradiances would be rescaled, as was done with the 1GP calculations studied here, and applied at the new grid point. If the IOPs at the

10647

new grid point differ by more than some amount from those at the reference point, then EcoLight would be called for a de novo calculation of the irradiance, and the current grid point would become the new reference point. A dynamic determination of when to call EcoLight would allow for frequent calls near fronts or in other situations where the IOPs or external properties are changing rapidly, and for few calls in fairly homogenous and stable ocean regions. When employed in this manner, EcoLight should be applicable to large-scale three-dimensional ecosystem models requiring spectral irradiances at many wavelengths and on a fine spatial and temporal grid, but at little more computational expense than calling an analytical light model at every time step and grid point, as is done in the current ROMS-EcoSim code.

Light is an important factor in determining primary production and mixed-layer thermodynamics, so we expect that EcoLight's accurately computed spectral scalar irradiances will significantly improve ecosystem model predictions, compared to the use of approximate analytical models for spectral irradiance or PAR. Moreover, predictions of primary production in shallow waters and for sea grass beds, for which analytic chlorophyll-based models can be off by large factors, would be well-served by the use of EcoLight.

The EcoLight version 1.0 code used in the present study is mostly Fortran 77 and contains HydroLight legacy features that are not needed for ecosystem simulations. We expect that a thorough rewriting of EcoLight in Fortran 95, removal of unneeded features, and use of a faster RTE solver might gain another factor of two in run times for the EcoLight module. That rewrite is now under way. When ready, that code will be imbedded in a fully 3-D ecosystem model for investigation of the issues just mentioned.

*Acknowledgements.* Authors C. D. M. and L. K. S. were supported in this work by the US Office of Naval Research Environmental Optics Program as part of the Hyperspectral Coastal Ocean Dynamics Experiment (HyCODE) and under follow-on contracts N00014-00-D-0161, N00014-05-M-0146, and N00014-8-C-0024. Authors W. P. B. and B. C. were supported by Office of Naval Research Environmental Optics Program as part of HyCODE, under follow-on contract N00014-8-C-0024, and by the US National Science Foundation Coastal Ocean Processes Lagrangian Transport and Transformation Experiment (LaTTE) under grant 0238745.

10648

## References

- Baker, K. S. and Frouin, R.: Relation between photosynthetically available radiation and total insolation at the ocean surface under clear skies, *Limnol. Oceanogr.*, 32, 1370–1377, 1987. 10629
- 5 Bissett, W. P., Meyers, M. B., Walsh, J. J., and Müller-Karger, F. E.: The effects of temporal variability of mixed layer depth on primary productivity around Bermuda, *J. Geophys. Res.*, 99(C4), 7539–7553, 1994. 10627
- Bissett, W. P., Walsh, J. J., Dieterle, D. A., and Carder, K. L.: Carbon cycling in the upper waters of the Sargasso Sea: I. Numerical simulation of differential carbon and nitrogen fluxes, *Deep-Sea Res.*, 46, 205–269, 1999a. 10629, 10632, 10633
- 10 Bissett, W. P., Carder, K. L., Walsh, J. J., and Dieterle, D. A.: Carbon cycling in the upper waters of the Sargasso Sea: II. Numerical simulation of apparent and inherent optical properties, *Deep-Sea Res.*, 46, 271–317, 1999b. 10629, 10632, 10634
- Bissett, W. P., Schofield, O., Glenn, S., Cullen, J. J., Miller, W. L., Plueddemann, A. J., and Mobley, C. D.: Resolving the impacts and feedbacks of ocean optics on upper ocean ecology. *Oceanography*, 14, 30–49, 2001. 15
- Bissett, W. P., DeBra, S., and Dye, D.: Ecological Simulation (EcoSim) 2.0 Technical Description. FERI Technical Document Number FERI-2004-0002-U-D, online available at: [http://feri.s3.amazonaws.com/pubs\\_ppts/FERI\\_2004\\_0002\\_U\\_D.pdf](http://feri.s3.amazonaws.com/pubs_ppts/FERI_2004_0002_U_D.pdf), 10 August, 2004. 10633
- 20 Bissett, W. P., Arnone, R., DeBra, S., Dieterle, D. A., Dye, D., Kirkpatrick, G., Schofield, O. M., and Vargo, G.: Predicting the optical properties of the West Florida Shelf: Resolving the potential impacts of a terrestrial boundary condition on the distribution of colored dissolved and particulate matter, *Mar. Chem.*, 95, 199–233, 2005. 10632
- Bissett, W. P., Arnone, R., DeBra, S., Dye, D., Kirkpatrick, G., Mobley, C. D., and Schofield, O. M.: The integration of ocean color remote sensing with coastal nowcast/forecast simulations of harmful algal blooms (HABs), in: *Real Time Coastal Observing Systems for Ecosystem Dynamics and Harmful Algal Blooms*, edited by: Babin, M., Roesler, C., and Cullen, J. J., UN Educ., Sci. and Cult. Organ., Paris, 85–108, 2008. 10632
- 25 Cahill, B., Schofield, O., Chant, R., Wilkin, J., Hunter, E., Glenn, S., and Bissett, W. P.: Dynamics of turbid buoyant plumes and the feedbacks on nearshore biogeochemistry and physics, *Geophys. Res. Lett.*, 35, L10605, doi:10.1029/2008GL033595, 2008. 10631
- Dinniman, M. S., Klinck, J. M., and Smith Jr., W. O.: Cross shelf exchange in a model of the 30
- Ross Sea circulation and biogeochemistry, *Deep-Sea Res. II*, 50, 3103–3120, 2003. 10631
- Doney, S. C., Glover, D. M., and Najjar, R. G.: A new coupled, one-dimensional biological-physical model for the upper ocean: Application to the JGOFS Bermuda Atlantic Timeseries Study (BATS) site, *Deep-Sea Res. II*, 43, 591–624, 1996. 10628
- 5 Eppley, R. W.: Temperature and phytoplankton growth in the sea, *Fish. Bull.*, 70(4), 1063–1085, 1972. 10632
- Evans, G. T. and Parslow, J. S.: A model of annual plankton cycles, *Biol. Oceanogr.*, 3, 328–347, 1985. 10627, 10628
- Fasham, M. J. R.: Variations in the seasonal cycle of biological production in subarctic oceans: A model sensitivity analysis, *Deep-Sea Res. II*, 42, 1111–1149, 1995. 10628
- 10 Fasham, M. J. R., Ducklow, H. W., and McKelvie, S. M.: A nitrogen-based model of plankton dynamics in the oceanic mixed layer, *J. Mar. Res.*, 48, 591–639, 1990. 10628
- Fennel, K. and Wilkin, J.: Quantifying biological carbon export for the northwest North Atlantic continental shelves, *Geophys. Res. Lett.*, in press, 2009. 10631
- 15 Fennel, K., Wilkin, J., Levin, J., Moisan, J., O'Reilly, J., and Haidvogel, D.: Nitrogen cycling in the Middle Atlantic Bight: Results from a three-dimensional model and implications for the North Atlantic nitrogen budget, *Global Biogeochem. Cy.*, 20, GB3007, doi:10.1029/2005GB002456, 2006. 10631
- Fennel, K., Wilkin, J., Previdi, M., and Najjar, R.: Denitrification effects on air-sea CO<sub>2</sub> flux in the coastal ocean: Simulations for the Northwest North Atlantic, *Geophys. Res. Lett.*, 35, L24608, doi:10.1029/2008GL036147, 2008. 10631
- 20 Fringer, O. B., McWilliams, J. C., and Street, R. L.: A new hybrid model for coastal simulations, *Oceanography*, 19, 64–77, 2006.
- Fujii, M., Boss, E., and Chai, F.: The value of adding optics to ecosystem models: a case study, *Biogeosciences*, 4, 817–835, 2007, <http://www.biogeosciences.net/4/817/2007/>. 10630
- Gordon, H. R. and Morel, A.: Remote assessment of ocean color for interpretation of satellite visible imagery, a review, *Lecture Notes on Coastal and Estuarine Studies*, 4, Springer Verlag, New York, 114 pp., 1983. 10634
- 30 Gregg, W. W. and Carder, K. L.: A simple spectral solar irradiance model for cloudless maritime atmospheres, *Limnol. Oceanogr.*, 35, 1657–1675, 1990. 10633
- Hurtt, G. C. and Armstrong, R. A.: A pelagic ecosystem model calibrated with BATS data, *Deep-Sea Res. II*, 43, 653–683, 1996. 10628

- Kywalyanga, M., Platt, T., and Sathyendranath, S.: Ocean primary production calculated by spectral and broad-band models, *Mar. Ecol.-Prog. Ser.*, 85, 171–185, 1992. 10628
- Liu, C.-C., Woods, J. D., and Mobley, C. D.: Optical model for use in oceanic ecosystem models, *Appl. Optics*, 38, 4475–4485, 1999. 10636
- 5 Liu, C.-C., Carder, K. L., Miller, R. L., and Ivey, J. E.: Fast and accurate model of underwater scalar irradiance, *Appl. Optics*, 41, 4962–4974, 2002. 10636
- Lutjeharms, J. R. E., Penven, P., and Roy, C.: Modelling the shear edge eddies of the southern Agulhas Current, *Cont. Shelf Res.*, 23, 1099–1115, 2003. 10631
- Marchesiello, P., McWilliams, J. C., and Shchepetkin, A. F.: Equilibrium structure and dynamics of the California Current System, *J. Phys. Oceanogr.*, 33(4), 753–783, 2003. 10631
- 10 Mobley, C. D.: *Light and Water: Radiative Transfer in Natural Waters*, Academic Press, San Diego, 1994. 10626, 10630, 10635, 10638
- Mobley, C. D., Gentili, B., Gordon, H. R., Jin, Z., Kattawar, G. W., Morel, A., Reinersman, P., Stamnes, K., and Stavn, R. H.: Comparison of numerical models for computing underwater light fields, *Appl. Optics*, 32, 7484–7504, 1993. 10630, 10635
- 15 Moore, J. K., Doney, S. C., Kleypas, J. A., Glover, D. M., and Fung, I. Y.: An intermediate complexity marine ecosystem model for the global domain, *Deep-Sea Res. II*, 49, 403–462, 2002. 10628
- Morel, A. and Maritorena, S.: Bio-optical properties of oceanic waters: a reappraisal, *J. Geophys. Res.*, 106(C4), 7163–7180, 2001. 10634
- 20 Oguz, T., Ducklow, H., Malanotte-Rizzoli, P., Tugrul, S., Nezlin, N. P., and Unluata, U.: Simulation of annual plankton productivity cycle in the Black Sea by a one-dimensional physical-biological model, *J. Geophys. Res.*, 101, 16585–16599, 1996. 10628
- Oschlies, A. and Garçon, V.: An eddy-permitting coupled physical-biological model of the North Atlantic - Part I: Sensitivity to advection numerics and mixed layer physics, *Global Biogeochem. Cy.*, 13, 135–160, 1998. 10628
- 25 Paulson, C. A. and Simpson, J. J.: Irradiance measurements in the upper ocean, *J. Phys. Oceanogr.*, 7, 952–956, 1977.
- Peliz, A., Dubert, J., Haidvogel, D. B., and Le Cann, B.: Generation and unstable evolution of a density-driven eastern poleward current: The Iberian Poleward Current, *J. Geophys. Res.*, 108(C8), 3268, doi:10.1029/2002JC001443, 2003. 10631
- 30 Sakshaug, E., Bricaud, A., Dandonneau, Y., Falkowski, P. G., Kiefer, D. A., Legendre, L., Morel, A., Parslow, J., and Takahashi, M.: Parameters of photosynthesis: definitions, theory, and

10651

- interpretation of results, *J. Plankton Res.*, 19, 1637–1670, 1997. 10627
- Shchepetkin, A. and McWilliams, J. C.: Quasi-monotone advection schemes based on explicit locally adaptive dissipation, *Mon. Weather Rev.*, 126, 1541–1580, 1998. 10631
- Shchepetkin, A. and McWilliams, J. C.: A method for computing horizontal pressure gradient force in an oceanic model with a nonaligned vertical coordinate, *J. Geophys. Res.*, 108, 3090, doi:10.1029/2001JC001047, 2003. 10631
- 5 Shchepetkin, A. F. and McWilliams, J. C.: The regional ocean modeling system (ROMS): a split-explicit, free-surface, topography-following-coordinate oceanic model, *Ocean Model.*, 9, 347–404, 2005. 10631
- 10 Simpson, J. J. and Dickey, T. D.: Alternative parameterizations of downward irradiance and their dynamical significance, *J. Phys. Oceanogr.*, 11, 876–882, 1981. 10629
- Steele, J. H. and Henderson, E. W.: The role of predation in plankton models, *J. Plankton Res.*, 14(1), 157–172, 1992. 10632
- 15 Wilkin, J. L.: The summertime heat budget and circulation of southeast New England shelf waters, *J. Phys. Oceanogr.*, 36(11), 1997–2011, 2006. 10631
- Zielinski, O., Oschlies, A., and Reuter, R.: Comparison of underwater light field parameterizations and their effect on a 1-dimensional biogeochemical model at Station ESTOC, north of the Canary Islands, in: *Proceedings Ocean Optics XIV, P. Soc. Photo-opt. Ins., Kona-Kailua, Hawaii*, 1998. 10628, 10629

10652

**Table 1.** Options used in comparison runs. Time resolution of 9 min is every ROMS time step; grid resolution of EGP is every ROMS grid point; wavelength resolution of 5 nm is every EcoSim wavelength. The run times are per year of simulation on a 2.16 GHz iMac computer.

model	time resolution	grid resolution	depth resolution $F_o$ of Eq.(6)	wavelength resolution	run time per simulation year hr:min
Analytic	9 min	EGP	NA	5 nm	0:32
EcoLight full	9 min	EGP	0.001	5 nm	135:35
EcoLight base	every hour	1 grid point	0.001	5 nm	8:34
EcoLight Run A	every 4 h	1 grid point	0.15	25 nm	0:41
EcoLight Run B	every 6 h	1 grid point	0.5	50 nm	0:40

10653

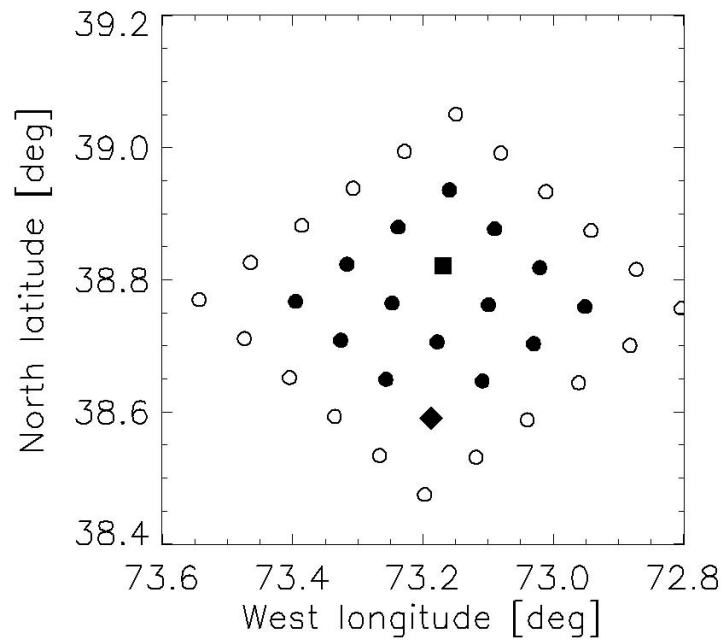


**Fig. 1.** The ROMS computational grid. The open circle grid points are used to apply the periodic boundary conditions. Biological computations are performed at the 4×4 interior grid shown by the solid symbols. Output in subsequent figures is plotted at the square. EcoLight runs that compute the light only at one grid point are done at the diamond.

10654

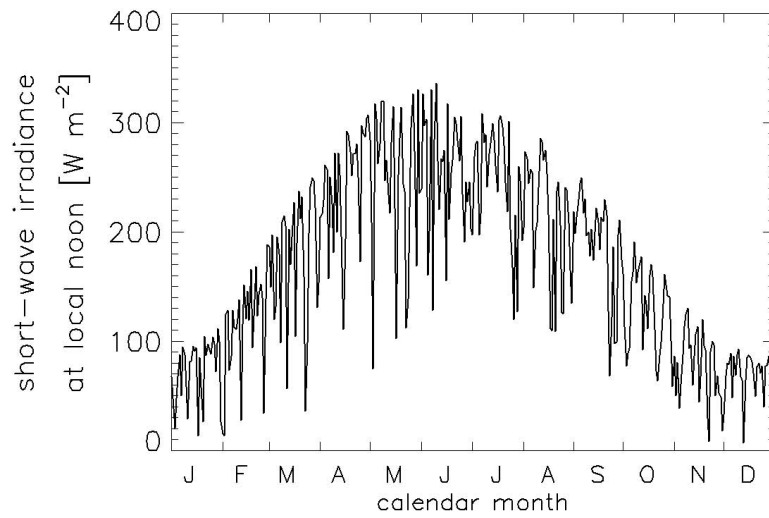


**Fig. 2.** Short-wave local-noon irradiances used in ROMS. This annual cycle was repeated for each year of the simulation.

10655

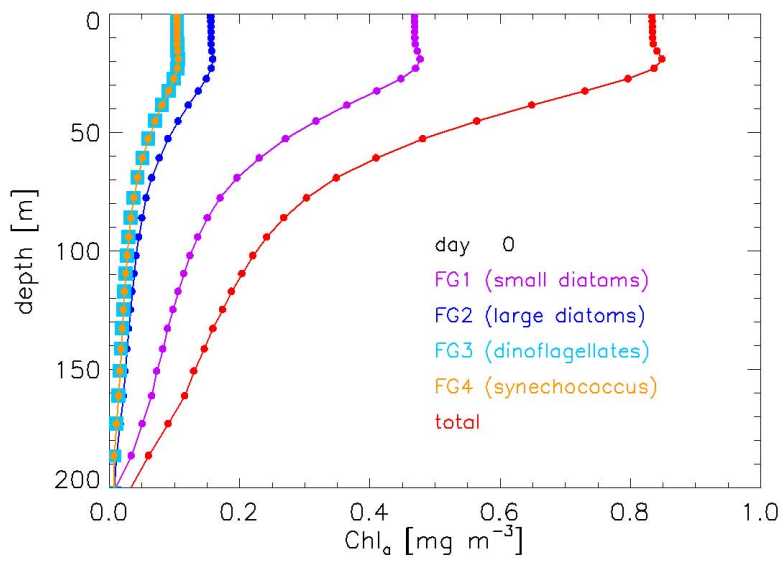


**Fig. 3.** The baseline initial depth profiles of Chl<sub>a</sub> for the four functional groups, and their total.

10656



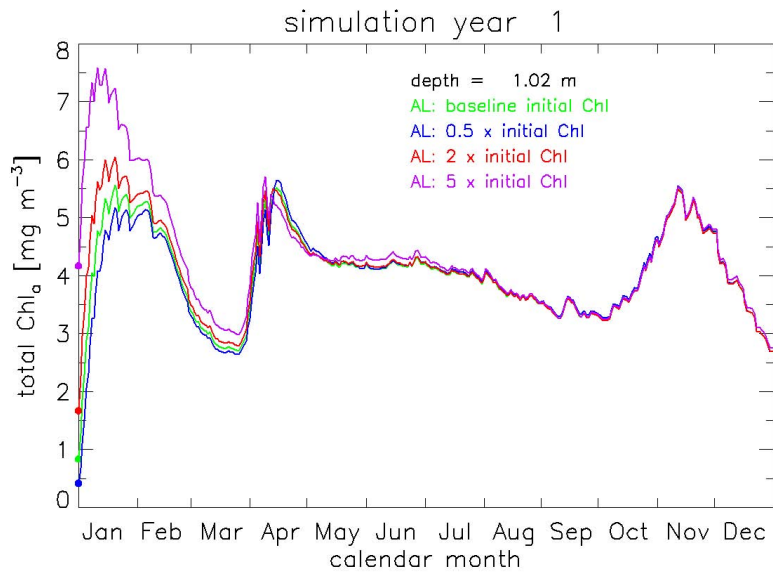


**Fig. 4.** Total near-surface chlorophyll values for one-year simulations starting with various initial chlorophyll depth profiles. Values are plotted daily at local noon.

10657

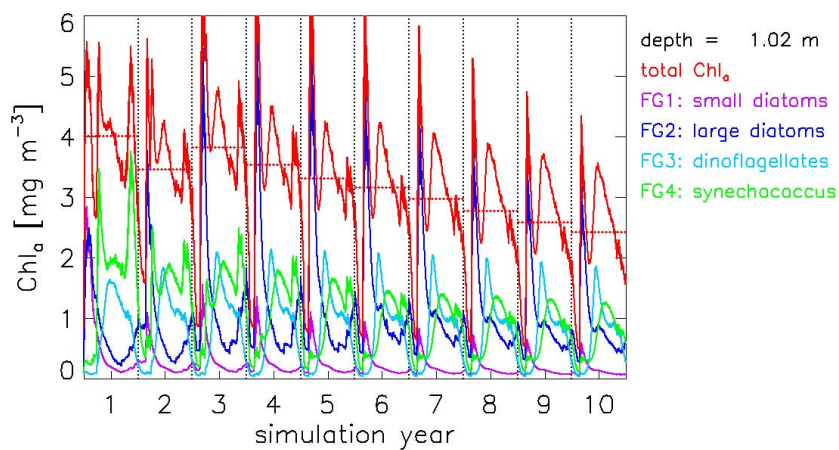


**Fig. 5.** Time series of surface chlorophyll for the ten-year baseline simulation using the analytic light model in EcoSim. The horizontal red dotted lines are the annual average total chlorophyll values within each simulation year. The vertical black dotted lines are at 31 December of each year.

10658

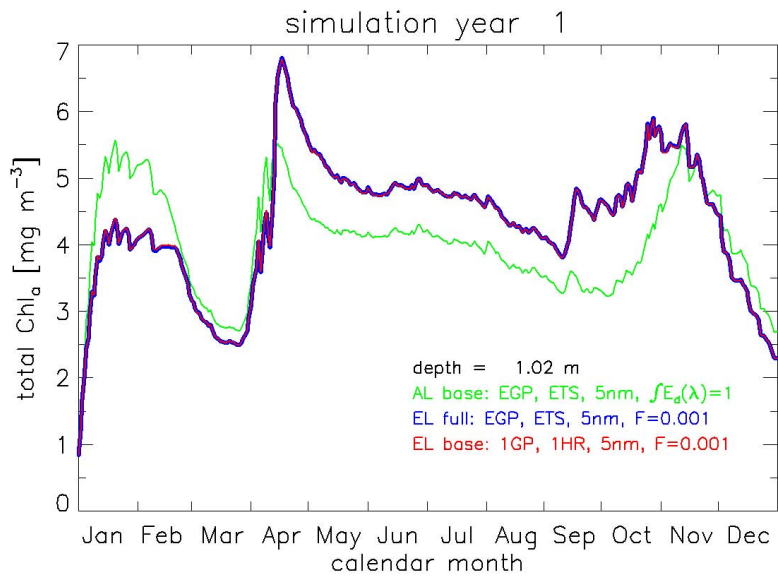


**Fig. 6.** Chlorophyll concentrations at depth of 1 m for various year 1 simulations as discussed in the text.

10659

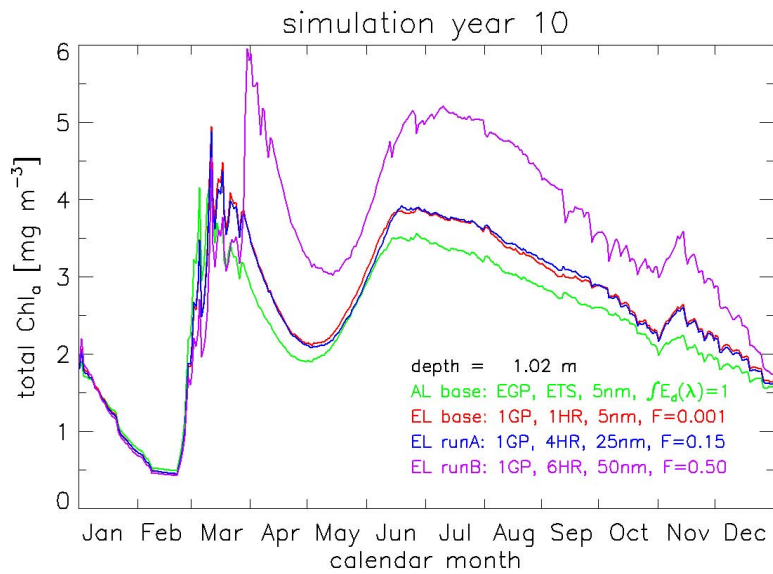


**Fig. 7.** Chlorophyll concentrations at depth of 1 m for various year 10 simulations as discussed in the text.

10660

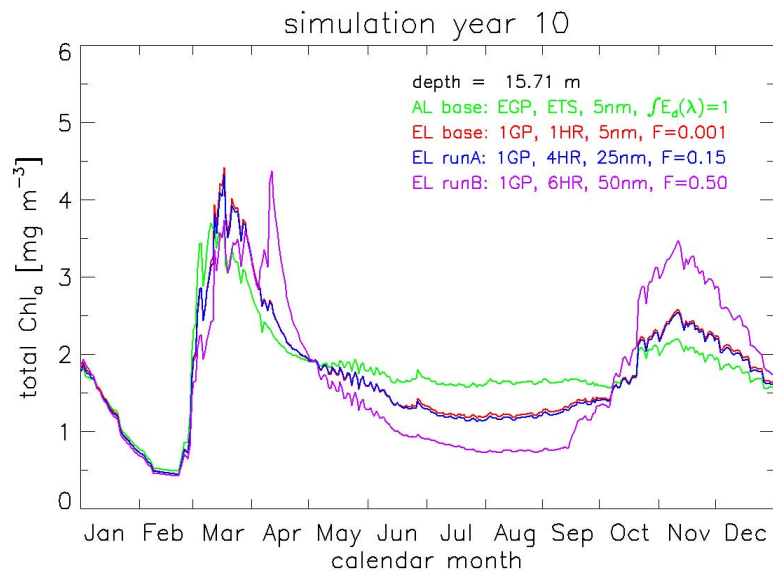


**Fig. 8.** Chlorophyll concentrations at depth of 15.7 m for various year 10 simulations as discussed in the text.

10661

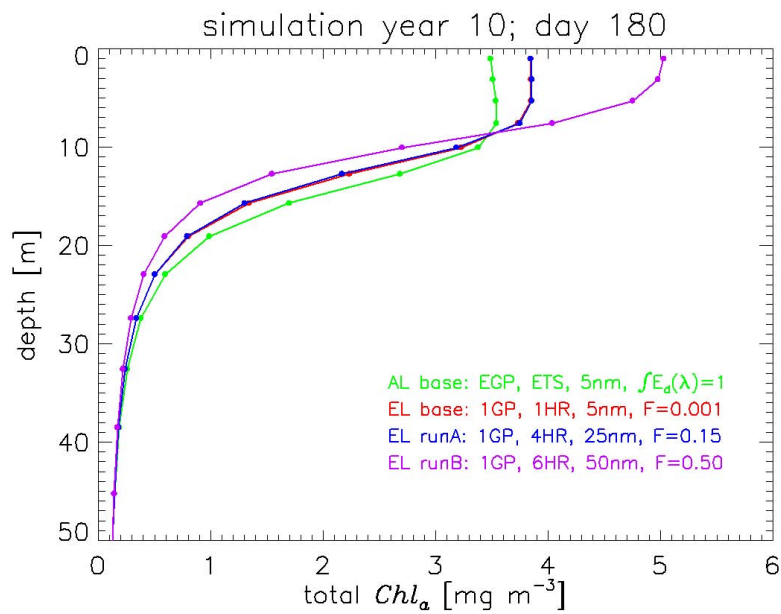


**Fig. 9.** Chlorophyll depth profiles corresponding to Figs. 7 and 8 at local noon of simulation day 180. The dots show the depths of the ROMS grid cell midpoints.

10662